

Efficient Online Learning of Contact Force Models for Connector Insertion

Kevin Tracy

KTRACY@CMU.EDU

Zachary Manchester

ZACM@CMU.EDU

The Robotics Institute, Carnegie Mellon University

Ajinkya Jain

AJINKYAJAIN@INTRINSIC.AI

Keegan Go

KEEGANGO@INTRINSIC.AI

Stefan Schaal

SSCHAAL@INTRINSIC.AI

[Google] Intrinsic

Tom Erez

ETOM@GOOGLE.COM

Yuval Tassa

TASSA@GOOGLE.COM

Google DeepMind Robotics

Abstract

Contact-rich manipulation tasks with stiff frictional elements like connector insertion are difficult to model with rigid-body simulators. In this work, we propose a new approach for modeling these environments by learning a quasi-static contact force model instead of a full simulator. Using a feature vector that contains information about the configuration and control, we find a linear mapping adequately captures the relationship between this feature vector and the sensed contact forces. A novel Linear Model Learning (LML) algorithm is used to solve for the globally optimal mapping in real time without any matrix inversions, resulting in an algorithm that runs in nearly constant time on a GPU as the model size increases. We validate the proposed approach for connector insertion both in simulation and hardware experiments, where the learned model is combined with an optimization-based controller to achieve smooth insertions in the presence of misalignments and uncertainty. Our website featuring videos, code, and more materials is available at <https://model-based-plugging.github.io/>.

Keywords: Adaptive control, system identification, Kalman Filter, connector insertion, online model learning

1. Introduction

Model-based control for robotic systems is incredibly effective when the model of the system is accurate (Tedrake, 2014). In many instances, the model can be made accurate through system identification, where experimental data is used with a parametrized physics model to estimate geometric, mass, contact, and friction properties (Galrinho, 2016; Hoburg and Tedrake, 2009). In scenarios where contact-free rigid-body dynamics accurately capture the behavior of the robot, system identification can enable highly performant model-based control. For robots in contact-rich settings where they make and break contact with the environment, system identification and simulation become much more challenging due to discontinuities and inevitable approximations in the physics modeling (Zhao et al., 2020).

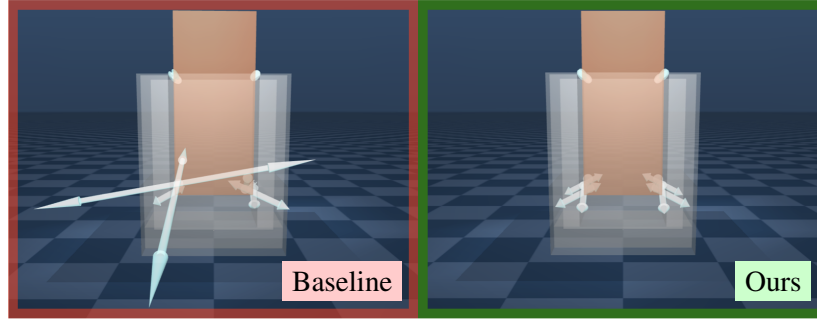


Figure 1: Inserting a significantly misaligned connector in MuJoCo, where a scripted insertion (left) results in large contact forces shown in white. During a short calibration sequence, a model is learned that predicts these contact forces as a function of the configuration of the connector and applied control wrench. A model-based controller is then able to solve for actions that minimize these forces and guide the connector to a smooth insertion (right). Our approach is fast, data efficient, robust to misalignments and uncertainty, and does not require any a priori knowledge of the plug.

Modern robotics simulators like MuJoCo (Todorov et al., 2012), Bullet (Coumans, 2015), Dart (Lee et al., 2018), Dojo (Howell et al., 2022), and Isaac Gym (Makoviychuk et al., 2021), approximate all bodies as rigid, where friction is either the idealized Coulomb friction or a closely related approximation. This results in a significant gap between simulation and reality, even with the use of system identification (Acary et al., 2018; Horak and Trinkle, 2019; Chatterjee; Elandt et al., 2019). Accurate simulation of contact-rich manipulation tasks is challenging due to deformability in the bodies, approximate geometries, and complex friction behavior not captured by Coulomb friction (Drumwright et al., 2010).

This paper focuses on the problem of robotic connector insertion, which displays rich contact interactions between a plug and its corresponding socket. This task is difficult to simulate accurately because of the precision required (being off by a millimeter results in jamming), and the contact/friction interactions between the two slightly deformable objects. The point-contact assumption that rigid-body simulators make begins to break down as the contact area dynamically changes. As a result, accurately simulating the insertion is challenging, and a policy that relies on the accuracy of this simulation is poorly suited for the diverse range of connectors available. Furthermore, even if a single connector style is modeled in great detail, there exists a significant amount of variability amongst connectors of the exact same specification.

The difficulty of the connector-insertion problem has motivated multiple approaches, some model-based and others model-free. The authors in Zhao et al. (2022) propose an offline model-free meta-reinforcement-learning algorithm to pre-train policies for insertion tasks using offline demonstration data and then adapt them to new tasks using online fine tuning. In Fu et al. (2023), the insertion is divided into an alignment phase and an insertion phase. During the alignment phase, a policy that relies on tactile feedback is used to line up the connector, and insertion is achieved with a separate RGB-image-based policy. In Nair et al. (2023), a simulation is used with domain randomization to train a robust policy over a wide variety of connectors, enabling generalization; and in Tang et al. (2023) a simulation-aware policy training style is used to prioritize experiences that align with the physics model. Alternatively, in Kang et al. (2022), a policy is used solely to generate a search pattern that systematically inserts connectors in the presence of model and state

uncertainty. In all of these approaches, significant time and effort must be devoted to offline training from experiments, making rapid adaptation to new plugs challenging.

In this work, we present a different approach to model-based connector insertion that relies on a learned quasi-static *contact-force model* instead of a full simulator. Many contact-rich robotic manipulation tasks can be assumed to be quasi-static, meaning the system moves slowly enough that the Coriolis forces and accelerations in the dynamics are small enough to be ignored (Mason, 2001; Halm and Posa, 2019). This approximation allows us to describe the state of the robot solely by its configuration (without velocity). When compared to full second-order dynamics simulation, quasi-static simulators are more stable, simpler, and have shown great promise for use in contact-rich manipulation planning (Pang et al., 2023; Suh and Tedrake, 2020).

When analyzing experimental data, a linear model with an engineered feature vector was found to be expressive enough to accurately predict contact forces on the connector during an insertion task. The linearity (in the features) of this model allows for an entirely decoupled model-learning process, where a novel Linear Model Learning (LML) filter is developed for learning the maximum a posteriori estimate to global optimality in a recursive fashion. The resulting algorithm is entirely free of matrix inversions, and the run time is nearly constant on a GPU as the size of the model increases. This model is then used in a convex-optimization-based control policy where the connector is smoothly inserted. The contributions of this paper include:

- A validated contact-force model that linearly maps a feature vector with information about the configuration and control to predicted force torque sensor values during a connector insertion.
- The Linear Model Learning (LML) algorithm that recursively updates the optimal estimated contact force model without any matrix inversions.
- A model-based controller that uses this contact force model to achieve smooth connector insertions.

2. Feature-Based Contact Force Model

Conventionally, physics simulations used in model-based control take the form of a discrete dynamics function $x_{k+1} = f(x_k, u_k)$, where the current state, x_k , and control, u_k , are used to calculate the state at the next time step, x_{k+1} . The state of the system, x , is normally comprised of a configuration, $q \in \mathbf{R}^{n_q}$, and velocity, $v \in \mathbf{R}^{n_v}$ (Tedrake, 2014). For systems modeled with standard rigid-body dynamics, the full second-order dynamics depend on both the configuration of the system as well as the velocity. However, for the damped, slow-moving systems common in contact-rich manipulation, velocity-dependent terms like Coriolis forces can be small enough to be effectively ignored (Mason, 2001). The quasi-static assumption also simplifies the actuator dynamics of impedance-controlled robots, where the behavior of the controller is directly incorporated as part of the model (Pang and Tedrake, 2018).

For quasi-static contact-rich tasks where the end effector of the robot is in constant contact with the environment, we can learn a contact-force model and still maintain all of the predictive power of a full simulator. To accurately represent the dynamics in this regime, all we need is a model that takes in the current configuration of the robot and applied control, and outputs the predicted force-torque sensor reading. With the ability to predict how the force-torque sensor responds to control inputs, a model-based controller is able to fully reason about the contact environment.

The model we seek to learn takes the configuration of the system, the control, $u \in \mathbf{R}^{n_u}$, and the contact force torque measurement, $\tilde{y} \in \mathbf{R}^{n_y}$ as inputs. Specifically, we are going to map the configuration and control into a feature vector, $w \in \mathbf{R}^{n_w}$, using an arbitrary mapping function,

$$w = \Omega(q, u), \quad (1)$$

after which we learn a *linear* mapping that transforms the feature vector into the predicted force, $f \in \mathbf{R}^3$, and torque, $\tau \in \mathbf{R}^3$, on the connector, $\tilde{y} = [f^T, \tau^T]^T \in \mathbf{R}^6$:

$$\tilde{y} \approx \tilde{G}w, \quad (2)$$

where $\tilde{G} \in \mathbf{R}^{n_y \times n_w}$. There are multiple benefits to representing our force model as a linear function of the feature vector, both in terms of system identification and control. For system identification, the resulting optimization problem is convex and can be solved to global optimality in real time with minimal computational cost. For control, as long as the feature vector in (1) is linear in u , the predicted force and torque can be minimized with convex optimization. This is true even in the presence of a feature vector that is highly nonlinear in q .

3. Linear Model Learning

Given data from a trajectory, a maximum-likelihood estimate (MLE) of the linear mapping \tilde{G} can be computed with numerical optimization by penalizing differences between the predicted and observed sensor measurements (Xinjilefu et al., 2014). To express this, we consider our contact force model from (2) with a force-torque sensor noise covariance $R \in \mathbf{S}_+^{n_y}$, and introduce the following optimization problem:

$$\underset{\tilde{G}}{\text{minimize}} \quad \sum_{k=1}^m \|\tilde{G}w_k - \tilde{y}_k\|_{R^{-1}}^2, \quad (3)$$

where the subscript k denotes the quantity from the k^{th} timestep, m is the length of the trajectory, and $\|\nu\|_{R^{-1}}^2 = \nu^T R^{-1} \nu$. It is worth pointing out that the primal variable in (3) is a matrix and not a vector, so it is not a canonical least squares problem. That being said, the linearity of the model still makes this an unconstrained convex optimization problem, where a closed-form solution exists (Boyd and Vandenberghe, 2004). However, for systems where the dimension of the feature vector is large, this problem can be both expensive to solve and numerically ill-conditioned when the trajectory is long (Benesty and Gansler, 2005).

There is a long history of solving variants of (3) from data, starting with the Ho-Kalman algorithm (Ho and Kalman, 1966) to more modern versions as shown in Galrinho (2016); Ghahramani; Hazan et al. (2017); Hardt et al. (2019). Instead of solving this problem directly, the following subsections walk through a method for decomposing (3) into a set of smaller decoupled problems that can be solved in parallel, as well as a recursive method for solving this problem online in a scalable and numerically robust way that completely avoids matrix inversions.

3.1. Decoupled Model Learning

The first step in decoupling (3) into a set of n_y smaller problems is to take a Cholesky decomposition of the inverse sensor covariance, R^{-1} , such that $R^{-1} = LL^T$, where $L \in \mathbf{R}^{n_y \times n_y}$ is the lower-

triangular Cholesky factor. From here, (3) can be re-written as the following:

$$\underset{\tilde{G}}{\text{minimize}} \quad \sum_{k=1}^m \|L^T \tilde{G} w_k - L^T \tilde{y}_k\|_2^2 \quad (4)$$

Next, we introduce new variables $G = L^T \tilde{G}$ and $y = L^T \tilde{y}$ that decouple each row of G and y from the others:

$$\underset{G}{\text{minimize}} \quad \sum_{k=1}^m \|G w_k - y_k\|_2^2, \quad (5)$$

where the solution to (4) can be recovered from the solution to (5) by simply transforming our matrix back with $\tilde{G} = L^{-T} G$. The inverse L^{-T} is computed once offline for a specific sensor and stored.

Next, we add regularization to the problem to improve conditioning and ensure that values in G are of reasonable magnitudes. To do this, a quadratic regularizer is added in the following manner:

$$\underset{G}{\text{minimize}} \quad \sum_{k=1}^m \|G w_k - y_k\|_2^2 + \|G b\|_2^2, \quad (6)$$

where $b \in \mathbf{R}^{n_w}$ contains the regularization weights. This allows for (6) to be decoupled into a set of n_y problems where each row of G is solved for entirely independently. The resulting optimization problem over the j^{th} row of G , and y can now be formulated:

$$\underset{g^{(j)}}{\text{minimize}} \quad \sum_{k=1}^m \|(g^{(j)})^T w_k - y_k^{(j)}\|_2^2 + (b^T g^{(j)})^2, \quad (7)$$

where the $g^{(j)}$ corresponds to the j^{th} row of G . This allows us to solve n_y parallel instances of (7) with n_w decision variables each, instead of one large problem with $n_y \cdot n_w$ variables. It is important to note that there are no approximations made between (6) and (7), and that they will always recover the same solution.

4. Linear Model Learning with a Kalman Filter

The problem posed in (7) is an unconstrained convex optimization problem whose solution can be computed by solving a single linear system, with a solution complexity that is cubic in the length of the feature vector, n_w . In scenarios where online, real-time system identification is desired, a recursive method can be used that updates the solution for each new sensor measurement. One option for solving (7) in a recursive fashion would be to use a standard Recursive Least Squares (RLS) algorithm. While this method can work, it has three major downsides: Long trajectories present numerical instability, adaptively updating the regularizer is expensive and approximate, and most importantly, there is no way to directly reason about process noise on the parameters (Liavas and Regalia, 1998, 1999; Benesty and Gansler, 2005).

To tackle these issues, we formulate our model-learning problem as a dynamical system and use a Kalman Filter to estimate each row of G independently. First, the connection between the canonical Kalman Filter and its corresponding optimization problem must be made (Kalman, 1960).

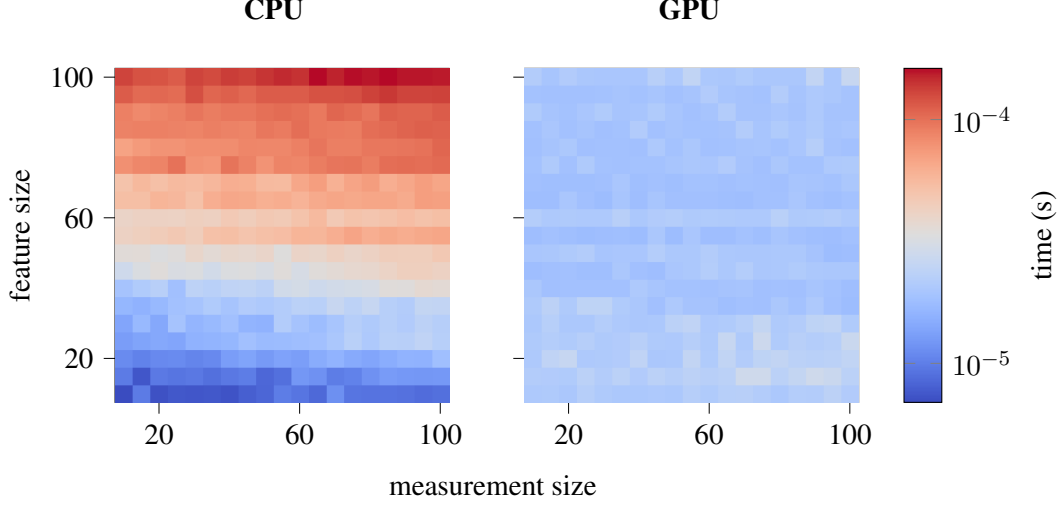


Figure 2: A comparison between run times of the LML algorithm on a CPU and an NVIDIA V100 GPU. The LML algorithm is comprised entirely of highly parallelizable operations (no matrix inversions), so the GPU is able to run the algorithm in constant time as the number of parameters in the model grows by a factor of 100.

For a canonical dynamical system with a state $x \in \mathbf{R}^{n_x}$ and measurement $z \in \mathbf{R}^{n_z}$, the dynamics and measurement functions are described by,

$$x_{k+1} = Ax_k + q_k, \quad q \sim \mathcal{N}(0, V), \quad (8)$$

$$z_k = Cx_k + r_k, \quad r \sim \mathcal{N}(0, W), \quad (9)$$

where q and r are the (unknown) process and sensor noises, and x is the (unknown) state being estimated. The Kalman Filter is then initialized with a Gaussian belief over the initial condition, $x_0 \sim \mathcal{N}(\mu_{ic}, \Sigma_{ic})$. Since the initial belief, the process noise, and the sensor noise are all assumed to be Gaussian, the maximum a posteriori (MAP) problem takes the form of an unconstrained convex quadratic program:

$$\underset{\mu_{0:m}}{\text{minimize}} \quad \|\mu_{ic} - \mu_0\|_{\Sigma_{ic}^{-1}}^2 + \sum_{k=0}^{m-1} \|\mu_{k+1} - A\mu_k\|_{Q^{-1}}^2 + \|z_{k+1} - C\mu_{k+1}\|_{R^{-1}}^2, \quad (10)$$

where the trajectory $\mu_{0:m}$ that minimizes the covariance-weighted errors in the dynamics, the sensor, and the initial belief is solved for. This is the optimization problem that the Kalman Filter solves (to global optimality) in a recursive fashion.

4.1. Parallelizing a Kalman Filter over Sensor Dimensions

We now convert our decoupled optimization problems from (7) into a form such that a Kalman Filter can be used to solve for the estimates of each of the n_y rows of G in parallel. From here, a common structure amongst these n_y filters allows us to handle the estimated G directly in a single, parallelizable LML algorithm in which the most expensive operations are matrix multiplications.

Algorithm 1: Linear Model Learning

Input: $\hat{G}_{k|k}, \Sigma_{k|k}, w_{k+1}, y_{k+1}$
 /* predict belief updates */
 $\hat{G}_{k+1|k} \leftarrow \hat{G}_{k|k}$
 $\Sigma_{k+1|k} \leftarrow \Sigma_{k|k} + Q$
 /* innovation and Kalman Gain */
 $z \leftarrow y_{k+1} - \hat{G}_{k+1|k} w_{k+1}$
 $s \leftarrow w_{k+1}^T \Sigma_{k+1|k} w_{k+1} + 1$
 $\ell \leftarrow \Sigma_{k+1|k} w_{k+1} / s$
 /* update mean and covariance */
 $\hat{G}_{k+1|k+1} \leftarrow \hat{G}_{k+1|k} + z \ell^T$
 $\Sigma_{k+1|k+1} \leftarrow (I - \ell w_{k+1}^T) \Sigma_{k+1|k} (I - \ell w_{k+1}^T) + \ell \ell^T$
Output: $\hat{G}_{k+1|k+1}, \Sigma_{k+1|k+1}$

Algorithm 2: Adaptive Regularization

Input: \hat{G}, Σ, ρ
for $i \leftarrow 1$ **to** n_w **do**
 $c \leftarrow 0_{n_w}$
 $c[i] \leftarrow 1$
 $r \leftarrow (1/\rho[i])^2$
 $s \leftarrow \Sigma[i, i] + r$
 $\ell \leftarrow \Sigma[:, i] / s$
 $\Sigma \leftarrow (I - \ell c^T) \Sigma (I - \ell c^T) + r \ell \ell^T$
 $\hat{G} \leftarrow \hat{G} - \hat{G}[:, i] \ell^T$
end
Output: \hat{G}, Σ

To start, the estimate of each row of G has its own Gaussian belief. Each of these n_y beliefs are represented with a mean estimate $\hat{g}^{(j)}$ and covariance $\Sigma^{(j)}$. From here, the discrete-time dynamics for the filter are:

$$g_{k+1}^{(j)} = g_k^{(j)} + q_k^{(j)}, \quad q_k^{(j)} \sim \mathcal{N}(0, Q), \quad (11)$$

where $q_k^{(j)} \in \mathbf{R}^{n_w}$ is the (unknown) additive Gaussian process noise, with a covariance of $Q \in \mathbf{S}_+^{n_w}$. This can also be interpreted as a more expressive version of a “forgetting factor”, where a non-zero process-noise covariance quantifies the expected change in parameters over the course of the experiment, therefore putting more emphasis on newer measurements than old.

The measurement function in the filter for row j is where we use the row parameters $g^{(j)}$ with our feature vector w to predict the j^{th} measurement:

$$y_k^{(j)} = w_k^T g_k^{(j)} + v_k, \quad v \sim \mathcal{N}(0, 1.0), \quad (12)$$

where $v \in \mathbf{R}$ is the (unknown) sensor noise with a variance of one, a result that comes from our change of variables in (5). Importantly, the measurement in (12) is a scalar, which means the computation of the Kalman Gain only requires the inversion of a scalar instead of a matrix:

$$\ell = (\Sigma w)(w^T \Sigma w + 1)^{-1} = \frac{\Sigma w}{w^T \Sigma w + 1}, \quad (13)$$

eliminating the only matrix inversion present in the Kalman Filter.

The dynamics and measurement equations in (11-12) are in the canonical form shown in (8-9), where $A = I$ and $C = w_k^T$. Critically missing from these matrices is any reference to row j , meaning the filters for all n_y rows have the same process and measurement functions. This enables two important commonalities amongst the n_y filters: They all share the same covariance and Kalman Gain. Therefore, we only need to maintain a single “global” covariance Σ that represents each of the n_y rows, and use the shared Kalman Gain, $\ell \in \mathbf{R}^{n_w}$ to update everything.

Using the Kalman Gain, the updates to the mean estimate of each row are:

$$\hat{g}_{k+1|k+1}^{(j)} = \hat{g}_{k+1|k}^{(j)} + \ell(y_{k+1}^{(j)} - \hat{g}_{k+1|k}^{(j)} w_{k+1}) \quad \forall j \in [1, n_y], \quad (14)$$

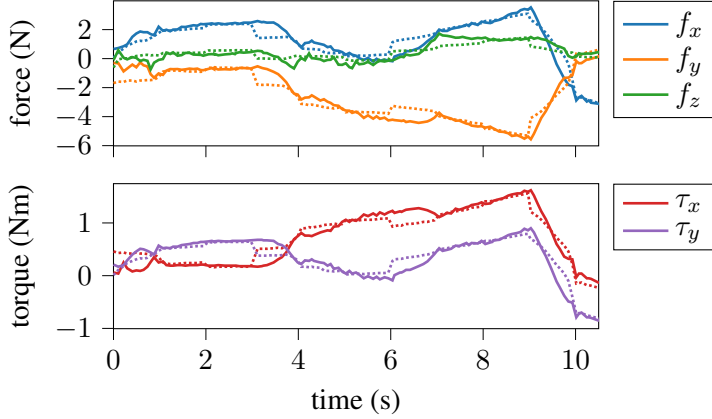


Figure 3: The sim-to-real gap for a connector insertion calibration sequence, where the real force torque sensor measurements are solid and the predicted measurements from our learned model are dotted. The learned model is able to accurately capture the contact force behavior of the connector inside the socket.

and since the Kalman Gain is shared, these individual row updates can be broadcast to an estimate of the full matrix \hat{G} :

$$\hat{G}_{k+1|k+1} = \hat{G}_{k+1|k} + (y_{k+1} - \hat{G}_{k+1|k} w_{k+1}) \ell^T, \quad (15)$$

where the parallelism is simply handled by a vector outer product and matrix addition. Using this technique on the parallel filters results in the LML algorithm, which is detailed in Algorithm 1.

Lastly, the regularization term from (7) must be included in the LML algorithm as an initialization. To do this, the cost terms associated with the initial Gaussian belief in the MAP problem (10) are adapted to replicate the regularization in (7) in the form of an initial Gaussian belief over row j :

$$\hat{g}_{0|0}^{(j)} = 0_{n_w}, \quad \Sigma_{0|0} = \text{diag}(1/b^2). \quad (16)$$

With this initialization, the LML algorithm is called recursively every time a new measurement is available. The entire algorithm is matrix-inversion free, requiring only simple matrix products and additions that are trivial to parallelize on a GPU. To demonstrate the importance of this, timing results of the LML algorithm run on a GPU and CPU are shown in Fig. 2, where the run time on a GPU stays constant as the number of parameters in \hat{G} grows by a factor of 100.

4.2. Adaptive Regularization

In the original cost function of (3), the relative importance of the regularization term is dependent on the trajectory length. As the trajectory gets longer, the impact the regularization has on the estimate decreases. In cases where the LML algorithm is being run for an unknown amount of time, choosing the appropriate regularizer offline is difficult. To deal with this, we present a method for updating the regularization term online that can handle arbitrary quadratic regularization and does not require any matrix inversions.

We specify this additional regularizer in a general form $\|G\rho\|_2^2$ that will be included in the cost function of (3). To add this to the LML algorithm, the connection between the MAP problem in (10) and the Kalman Filter is used once again. As before, we formulate a fictitious measurement equation for each $\hat{g}^{(j)}$ such that we recover the quadratic regularizer in the MAP cost, then use the same parallelization strategy to generalize it to \hat{G} .

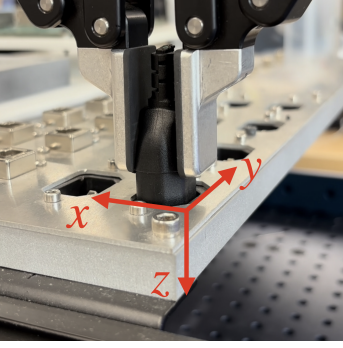


Figure 4: Calibration and insertion of a power plug into a socket with a Franka robot arm and parallel gripper.

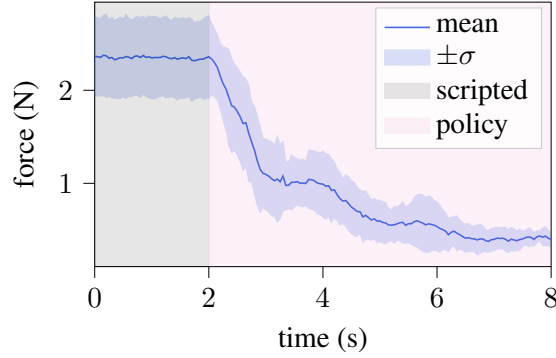


Figure 5: Magnitude of the force on the plug in the XY axis during insertion of eight different plugs. The scripted insertion leaves a constant force on the plug, after which the policy is used to reduce the force on the connector.

Our estimated mean $\hat{g}^{(j)}$ will have stationary dynamics, but we use a measurement function where each row has the values of the row j returned,

$$z_k = \hat{g}_k^{(j)} + r_k. \quad (17)$$

By expecting this “measurement” to be zero, we use our regularizer as a covariance for the fictitious sensor, $r \sim \mathcal{N}(0, \text{diag}(1/\rho^2))$, reconstructing our desired regularization cost in the MAP problem. Normally the Kalman Filter requires a matrix the size of the measurement to be inverted, however, since this fictitious sensor noise is diagonal, we can use the method of sequential scalar measurement updates to once again avoid any matrix inversions (Kailath et al., 2000). Similar to the LML algorithm, these operations can be broadcast to each row of G using matrix multiplication, as shown in Algorithm 2.

5. Experiments

We demonstrate LML algorithm on a contact-rich connector-insertion task, where the resulting contact-force model is used in a convex-optimization control policy. This approach is first shown to work in simulation with MuJoCo, then on hardware with a Franka robot arm with a parallel gripper holding a standard C13 power plug.

To learn the relationship between the configuration, control, and contact wrench on the plug, the LML algorithm will be used with the following feature vector:

$$w = \text{vcat}(r, \text{vec}(R), r_{des}, \phi, 1), \quad (18)$$

where $r \in \mathbf{R}^3$ is the cartesian position of the end effector, $R \in \mathbf{SO}(3)$ is the rotation matrix describing the attitude of the end effector, $r_{des} \in \mathbf{R}^3$ is the desired position sent to an impedance controller, $\phi \in \mathbf{R}^3$ is the axis-angle rotation between current attitude and desired attitude, and the 1 is included to account for a constant bias. The control inputs in this feature vector are r_{des} and ϕ , where the axis-angle parameterization is used to avoid any attitude-related constraints (Jackson et al., 2021).

The LML algorithm learns a linear relationship between this feature vector and the force torque sensor, $y \approx Gw$. To do this, a calibration sequence is run where both the position and attitude are varied. The force-torque sensor measurements and feature vectors are input to the LML algorithm during this calibration, and the resulting estimated sensor measurements are able to closely align with the true sensor measurements as shown in Fig. 3. To align the connector for insertion, a model-based controller uses this linear relationship to solve for controls that minimize the resistance measured by the force-torque sensor. The controller is posed as the solution to the following optimization problem:

$$\begin{aligned} & \underset{r_{des}, \phi}{\text{minimize}} && \|S\hat{y}\|_2^2 + \lambda\|r - r_{des}\|_2^2 + \mu\|\phi\|_2^2 \\ & \text{subject to} && \hat{y} = G[r^T, \text{vec}(R)^T, r_{des}^T, \phi^T, 1]^T, \\ & && \|r - r_{des}\|_\infty \leq 1 \text{ cm}, \\ & && \|\phi\|_\infty \leq 3^\circ, \end{aligned} \tag{19}$$

where $S = \text{diag}([1, 1, 0, 1, 1, 1])$ is used to penalize all forces and torques except for force in the Z (plug insertion) direction, $\lambda \in \mathbf{R}^+$ and $\mu \in \mathbf{R}^+$ are regularization weights, and the primal constraints ensure the commanded end-effector pose doesn't deviate too far from the current pose. Due to the linearity of our model, this problem is a small convex quadratic program, for which there are many available solvers for fast online execution (Mattingley and Boyd, 2012). We have found that a solver is not necessary since the controls can be sub-optimally clipped in the rare case the constraints are violated.

This system-identification and control strategy was first demonstrated in MuJoCo, as seen in Fig. 1, where the controller was successfully able to align the plug with initial misalignments. Second, a Franka robot arm with a parallel gripper was able to insert the C13 power plug into eight different sockets in the presence of misalignment, sensor noise, and actuator uncertainty. In both of these scenarios, LML was run on the force-torque sensor data during a quick 10-second calibration sequence, after which the controller was turned on and smooth insertion was achieved. On the Franka, the forces on the plug during these eight alignments are shown in Fig. 5, where the forces from the initial misalignment are dramatically reduced by over 80% once the controller takes over.

6. Conclusion

This work proposes a new approach for the modeling and control of connector-insertion tasks, where an estimated quasi-static contact model is used to predict the contact forces on the connector as a function of the configuration and control. This contact force model is learned online to global optimality with a novel Linear Model Learning algorithm that is free of matrix inversions. The runtime of this algorithm is shown to be constant on a GPU as the model size increases, since it is entirely comprised of parallelizable operations. The effectiveness of this modeling strategy is demonstrated both in simulation and in hardware experiments, where the contact-force model is used to solve for an optimal alignment policy for C13 power connectors.

References

- Vincent Acary, Maurice Brémond, and Olivier Huber. On Solving Contact Problems with Coulomb Friction: Formulations and Numerical Comparisons. In Remco Leine, Vincent Acary, and Olivier Brûls, editors, *Advanced Topics in Nonsmooth Dynamics*, pages 375–457. Springer International Publishing, Cham, 2018. ISBN 978-3-319-75971-5 978-3-319-75972-2. doi: 10.1007/978-3-319-75972-2_10.
- J. Benesty and T. Gansler. A recursive estimation of the condition number in the RLS algorithm [adaptive signal processing applications]. In *Proceedings. (ICASSP '05). IEEE International Conference on Acoustics, Speech, and Signal Processing, 2005.*, volume 4, pages iv/25–iv/28 Vol. 4, March 2005. doi: 10.1109/ICASSP.2005.1415936.
- Stephen Boyd and Lieven Vandenbergh. *Convex Optimization*. Cambridge University Press, 2004.
- Anindya Chatterjee. On the Realism of Complementarity Conditions in Rigid Body Collisions. page 10.
- Erwin Coumans. Bullet Physics Simulation. In *SIGGRAPH*, Los Angeles, 2015. ACM. ISBN 978-1-4503-3634-5. doi: 10.1145/2776880.2792704.
- Evan Drumwright, Dylan A. Shell, Evan Drumwright, and Dylan A. Shell. Modeling Contact Friction and Joint Friction in Dynamic Robotic Simulation Using the Principle of Maximum Dissipation. In Frans Groen, David Hsu, Volkan Isler, Jean-Claude Latombe, and Ming C. Lin, editors, *Workshop on the Algorithmic Foundations of Robotics (WAFR)*, Singapore, 2010. ISBN 978-3-642-17451-3 978-3-642-17452-0. doi: 10.1007/978-3-642-17452-0_15.
- Ryan Elandt, Evan Drumwright, Michael Sherman, and Andy Ruina. A pressure field model for fast, robust approximation of net contact force and moment between nominally rigid objects. *arXiv:1904.11433 [cs]*, April 2019.
- Letian Fu, Huang Huang, Lars Berscheid, Hui Li, Ken Goldberg, and Sachin Chitta. Safe Self-Supervised Learning in Real of Visuo-Tactile Feedback Policies for Industrial Insertion, March 2023.
- Miguel Galrinho. Least Squares Methods for System Identification of Structured Models. 2016.
- Zoubin Ghahramani. Parameter Estimation for Linear Dynamical Systems.
- Mathew Halm and Michael Posa. A Quasi-static Model and Simulation Approach for Pushing, Grasping, and Jamming, February 2019.
- Moritz Hardt, Tengyu Ma, and Benjamin Recht. Gradient Descent Learns Linear Dynamical Systems, February 2019.
- Elad Hazan, Karan Singh, and Cyril Zhang. Learning Linear Dynamical Systems via Spectral Filtering, November 2017.

- B L. Ho and R. E. Kalman. Editorial: Effective construction of linear state-variable models from input/output functions: Die Konstruktion von linearen Modeilen in der Darstellung durch Zustandsvariable aus den Beziehungen für Ein- und Ausgangsgrößen. *at - Automatisierungstechnik*, 14(1-12):545–548, December 1966. ISSN 2196-677X. doi: 10.1524/auto.1966.14.112.545.
- Warren Hoburg and Russ Tedrake. System Identification of Post Stall Aerodynamics for UAV Perching. In *AIAA Infotech@Aerospace Conference*. American Institute of Aeronautics and Astronautics, 2009.
- Peter C. Horak and Jeff C. Trinkle. On the Similarities and Differences Among Contact Models in Robot Simulation. *IEEE Robotics and Automation Letters*, 4(2):493–499, April 2019. ISSN 2377-3766, 2377-3774. doi: 10.1109/LRA.2019.2891085.
- Taylor A. Howell, Simon Le Cleac’h, J. Zico Kolter, Mac Schwager, and Zachary Manchester. Dojo: A Differentiable Physics Engine for Robotics. *IEEE Transactions on Robotics and Automation (In Review)*, June 2022. doi: 10.48550/arXiv.2203.00806.
- Brian E Jackson, Kevin Tracy, and Zachary Manchester. Planning with Attitude. *IEEE Robotics and Automation Letters*, January 2021.
- Thomas Kailath, Ali H. Sayed, and Babak Hassibi. *Linear Estimation*. Prentice Hall, 2000. ISBN 978-0-13-022464-4.
- R. E. Kalman. A New Approach to Linear Filtering and Prediction Problems. *Journal of Basic Engineering*, 82(1):35–45, March 1960. ISSN 0021-9223. doi: 10.1115/1.3662552.
- Hanwen Kang, Yaohua Zang, Xing Wang, and Yaohui Chen. Uncertainty-Driven Spiral Trajectory for Robotic Peg-in-Hole Assembly. *IEEE Robotics and Automation Letters*, 7(3):6661–6668, July 2022. ISSN 2377-3766. doi: 10.1109/LRA.2022.3176718.
- Jeongseok Lee, Michael X. Grey, Sehoon Ha, Tobias Kunz, Sumit Jain, Yuting Ye, Siddhartha S. Srinivasa, Mike Stilman, and C. Karen Liu. DART: Dynamic Animation and Robotics Toolkit. *The Journal of Open Source Software*, 3(22):500, February 2018. ISSN 2475-9066. doi: 10.21105/joss.00500.
- A.P. Liavas and P.A. Regalia. Numerical stability issues of the conventional recursive least squares algorithm. In *Proceedings of the 1998 IEEE International Conference on Acoustics, Speech and Signal Processing, ICASSP ’98 (Cat. No.98CH36181)*, volume 3, pages 1409–1412 vol.3, May 1998. doi: 10.1109/ICASSP.1998.681711.
- A.P. Liavas and P.A. Regalia. On the numerical stability and accuracy of the conventional recursive least squares algorithm. *IEEE Transactions on Signal Processing*, 47(1):88–96, January 1999. ISSN 1941-0476. doi: 10.1109/78.738242.
- Viktor Makoviychuk, Lukasz Wawrzyniak, Yunrong Guo, Michelle Lu, Kier Storey, Miles Macklin, David Hoeller, Nikita Rudin, Arthur Allshire, Ankur Handa, and Gavriel State. Isaac Gym: High Performance GPU-Based Physics Simulation For Robot Learning, August 2021.
- Matthew T. Mason. *Mechanics of Robotic Manipulation*. The MIT Press, June 2001. ISBN 978-0-262-25662-9. doi: 10.7551/mitpress/4527.001.0001.

- Jacob Mattingley and Stephen Boyd. CVXGEN: A code generator for embedded convex optimization. In *Optimization Engineering*, pages 1–27, 2012.
- Ashvin Nair, Brian Zhu, Gokul Narayanan, Eugen Solowjow, and Sergey Levine. Learning on the Job: Self-Rewarding Offline-to-Online Finetuning for Industrial Insertion of Novel Connectors from Vision, February 2023.
- Tao Pang and Russ Tedrake. A Robust Time-Stepping Scheme for Quasistatic Rigid Multibody Systems. In *2018 IEEE/RSJ International Conference on Intelligent Robots and Systems (IROS)*, pages 5640–5647, Madrid, October 2018. IEEE. ISBN 978-1-5386-8094-0. doi: 10.1109/IROS.2018.8594378.
- Tao Pang, H. J. Terry Suh, Lujie Yang, and Russ Tedrake. Global Planning for Contact-Rich Manipulation via Local Smoothing of Quasi-dynamic Contact Models, February 2023.
- H. J. Terry Suh and Russ Tedrake. The Surprising Effectiveness of Linear Models for Visual Foresight in Object Pile Manipulation. *Springer Proceedings in Advanced Robotics*, 17:347–363, February 2020. doi: 10.48550/arxiv.2002.09093.
- Bingjie Tang, Michael A. Lin, Iretiayo Akinola, Ankur Handa, Gaurav S. Sukhatme, Fabio Ramos, Dieter Fox, and Yashraj Narang. IndustReal: Transferring Contact-Rich Assembly Tasks from Simulation to Reality, May 2023.
- Russ Tedrake. Underactuated Robotics: Algorithms for Walking, Running, Swimming, Flying, and Manipulation (Course Notes for MIT 6.832). Technical report, Downloaded in Fall, 2014 from <http://people.csail.mit.edu/russt/underactuated/>, 2014.
- E. Todorov, T. Erez, and Y. Tassa. MuJoCo: A physics engine for model-based control. In *2012 IEEE/RSJ International Conference on Intelligent Robots and Systems*, pages 5026–5033, October 2012. doi: 10.1109/IROS.2012.6386109.
- X Xinjilefu, Siyuan Feng, and Christopher G. Atkeson. Dynamic state estimation using Quadratic Programming. In *2014 IEEE/RSJ International Conference on Intelligent Robots and Systems*, pages 989–994, Chicago, IL, USA, September 2014. IEEE. ISBN 978-1-4799-6934-0 978-1-4799-6931-9. doi: 10.1109/IROS.2014.6942679.
- Tony Z. Zhao, Jianlan Luo, Oleg Sushkov, Rugile Pevceviciute, Nicolas Heess, Jon Scholz, Stefan Schaal, and Sergey Levine. Offline Meta-Reinforcement Learning for Industrial Insertion, September 2022.
- Wenshuai Zhao, Jorge Peña Queralta, and Tomi Westerlund. Sim-to-Real Transfer in Deep Reinforcement Learning for Robotics: A Survey. In *2020 IEEE Symposium Series on Computational Intelligence (SSCI)*, pages 737–744, December 2020. doi: 10.1109/SSCI47803.2020.9308468.